World Electric Vehicle Journal

MDPI

Article

A Stator Fault Diagnosis Method Based on the Offline Motor Parameter Measurement for PMSM

Jing Tang [1], Chao Liang [1], Yuanhang Wang [1,2,*], Shuhan Lu [1] and Jian Zhou [1]

[1] The Fifth Electronics Research Institute of Ministry of Industry and Information Technology, Guangzhou 511370, China; tangjing1@ceprei.com (J.T.); msdn1988@163.com (C.L.); 15877250759@163.com (S.L.); zj20111018111@163.com (J.Z.)

[2] Guangdong Provincial Key Laboratory of Electronic Information Products Reliability Technology, Guangzhou 511370, China

* Correspondence: wangyuanhang@ceprei.com; Tel.: +86-131-6129-4848

Abstract: The permanent magnet synchronous motor (PMSM) is used widely in electric vehicle application due to its high-power density and efficiency. Stator fault is a frequently fault in the motor as it usually works in a harsh environment. Therefore, a stator fault diagnosis method based on the offline motor parameter measurement is proposed to detect and evaluate the stator fault in this paper. Firstly, the line-to-line resistance and inductance of a healthy motor are analyzed when a DC voltage and a high-frequency voltage are excited to the motor respectively, where the DC and AC equivalent circuits at a standstill are introduced. Then, to analyze the resistance and inductance of the stator fault, an extra branch is added to the fault part to obtain the fault equivalent circuits. Accordingly, the stator fault resistance and inductance are derived, and then the resistance and inductance differences between healthy and fault motors are analyzed to provide the basis for the stator fault detection. Furthermore, the fault indicators are defined based on the resistance and inductance differences when a motor has a stator fault. Hence the stator fault severity and location can be evaluated by using these fault indicators. Finally, the experimental results from a 400 W permanent magnet synchronous motor are demonstrated to validate the proposed method.

Keywords: stator fault; resistance; inductance; offline; PMSM

Citation: Tang, J.; Liang, C.; Wang, Y.; Lu, S.; Zhou, J. A Stator Fault Diagnosis Method based on the Offline Motor Parameter Measurement for PMSM. *World Electr. Veh. J.* **2021**, *12*, 248. https://doi.org/10.3390/wevj12040248

Academic Editor: Hui Yang

Received: 25 September 2021
Accepted: 17 November 2021
Published: 20 November 2021

1. Introduction

The permanent magnet synchronous motor (PMSM) is highly valued as well as widely used in electric vehicles, rail transit, and intelligent manufacturing due to its advantages of high-power density, efficiency, power factor, and small size [1,2]. However, the motors usually work in a harsh environment, leading to their failure. In serious cases, motor fault causes human life losses and material damages. Therefore, it is very important to discover and process early motor faults timely. Stator faults account for almost half of motor faults [3,4]. Reference [5] indicates that stator inter-turn short circuit fault is the primary cause of most stator faults, e.g., phase-to-phase and phase-to-ground faults. Hence, many stator inter-turn short circuit fault diagnosis methods have been developed.

To detect the stator inter-turn short circuit fault at an early stage, the offline and online stator fault diagnosis methods have been investigated [6–13]. The online method is very popular for research as it can monitor motor condition continuously and make failure prognosis in real time [6]. Due to the stator asymmetry of the fault, the negative sequence component will be produced in a motor current. In reference [7,8], the negative sequence in a motor current is adopted to detect the stator inter-turn short circuit fault. However, the inherent asymmetry and voltage unbalance can produce a negative sequence current as well, which will lead to a false alarm. Furthermore, the negative sequence impedance is developed [8,9]. Nevertheless, it is difficult to obtain accurate negative-sequence impedance for an inverter-fed PMSM, because the motor frequency changes with the vehicle speed

and contains several harmonics in a motor current. Moreover, the artificial intelligence (AI)-based method is attracting more and more attention in fault diagnosis application. The AI-based method usually classifies the failure types, fault severity and location, where the neural network (NN) [10], modular neural network (MNN) [11], classification and regression tree (CART) [12], k-nearest neighbors (k-NNs) [13], and multilayer perceptron (MLP) [13] are adopted to detect the stator fault. However, the accuracy of the AI-based method heavily depends on training data, which limits its application in practice.

Compared to the online stator fault diagnosis method, the offline method has the advantages of accuracy and being immune to motor running condition. Reference [14] summarizes different offline test methods, including overvoltage (hi-pot), the insulation resistance and polarization index (PI) test, voltage surge (surge comparison), power factor (PF) and PF tip-up, and PD. However, most offline tests need to supply a high voltage to the motor, which may further damage stator insulation.

To detect the stator fault easily and safely, this paper proposes a stator inter-turn short circuit fault diagnosis method by analyzing the line-to-line resistance and inductance, which has advantages of easy implementation and high accuracy. The rest of this paper is organized as follows: Section 2 analyzes the line-to-line resistance and inductance of a healthy motor through the equivalent circuit. In Section 3, an extra branch with R_f is added to the fault part, and thus the fault model is built to obtain the resistance and inductance under fault. Section 4 compares the resistance and inductance of the health and fault motor, and then the fault indicators are introduced to detect and locate the stator fault. In Section 5, the proposed fault diagnosis methods are validated through test results.

2. Line-to-Line Resistance and Inductance Analysis of a Healthy Motor

2.1. Line-to-Line Resistance Analysis

A DC voltage is applied to phases A and B of the motor, the equivalent is displayed in Figure 1, where U and I represent the DC voltage and current, respectively, R_A, R_B and R_C are the stator resistances of phases A, B and C, respectively. For simplicity, it gives the assumption that the motor is symmetrical for a healthy PMSM, i.e., $R_A = R_B = R_C = R_s$. Hence the line-to-line resistance between any two phases of the motor can be calculated as Equation (1) according to the equivalent circuit.

$$R_{AB} = R_{CA} = R_{BC} = 2R_s = \frac{U}{I} \tag{1}$$

where R_{AB}, R_{CA}, and R_{BC} are the line-to-line resistances of any two phases of the stator.

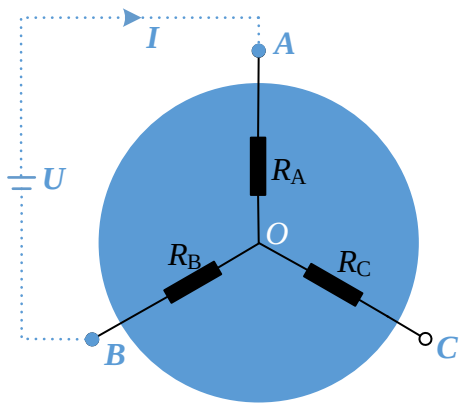

Figure 1. Equivalent circuit when a DC voltage is excited to phase A and B of a healthy motor.

2.2. Line-to-Line Inductance Analysis

When a low-magnitude and high-frequency AC voltage is applied to phases A and B, the motor remains stationary, and then the equivalent is displayed in Figure 2. In the figure, ψ_{AB} is the flux between A and B, i_{AB} is the current that flows through phases A

and B, i_A and i_B are the current of phases A and B, respectively, and L_{AA}, L_{BB} and L_{CC} are the self-inductances of phases A, B and C, respectively. Here, the AC frequency is high (>400 Hz) to ensure $\omega L >> R$. Hence the stator resistances can be ignored relative to the inductance.

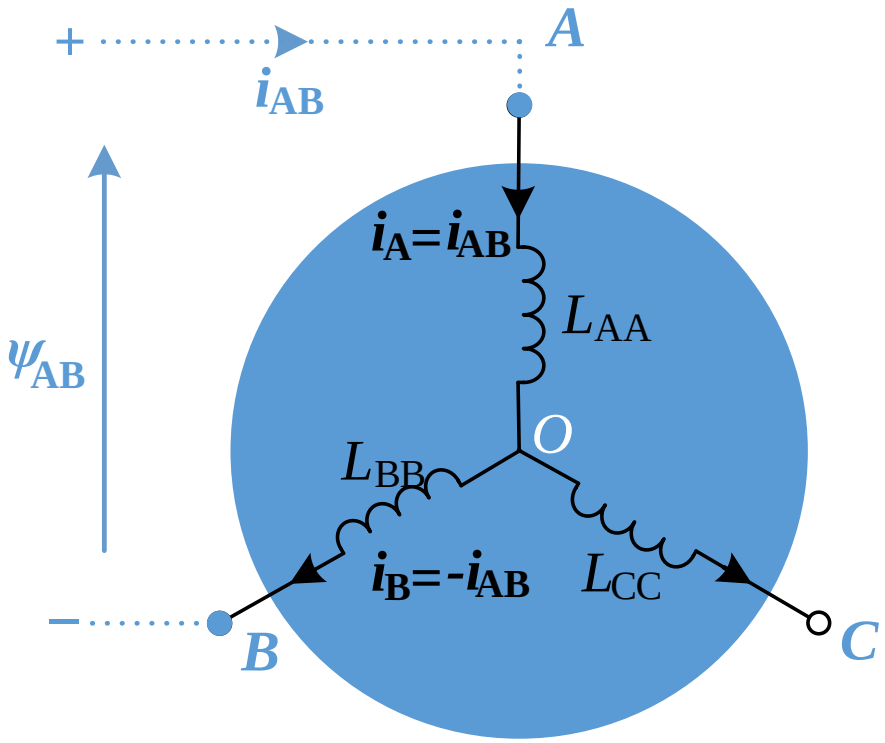

Figure 2. Equivalent circuit when a high frequency AC voltage is applied to phase A and B of a healthy motor.

According to the equivalent circuit, the flux of phase A and B can be calculated as

$$\begin{cases} \psi_A = (L_{AA} - L_{AB}) i_{AB} \\ \psi_B = (L_{AB} - L_{BB}) i_{AB} \end{cases} \tag{2}$$

where ψ_A and ψ_B are the flux of phase A and B respectively, L_{AB} is the mutual-inductance between phases A and B. Then, the ψ_{AB} can be derived as

$$\begin{aligned} \psi_{AB} &= \psi_A - \psi_B \\ &= (L_{AA} + L_{BB} - 2L_{AB}) i_{AB} \end{aligned} \tag{3}$$

Hence, the line-to-line inductance L_{AB}^{eq} can be expressed as (4) when the AC voltage is injected to the motor.

$$L_{AB}^{eq} = \frac{\psi_{AB}}{i_{AB}} = L_{AA} + L_{BB} - 2L_{AB} \tag{4}$$

where L_{AB}^{eq} represents the line-to-line inductance between phase A and B to distinguish the symbol from the mutual inductance L_{AB}. Similarly, when the AC voltage is applied to other phases, the line-to-line inductance is expressed as:

$$\begin{cases} L_{AB}^{eq} = L_{AA} + L_{BB} - 2L_{AB} \\ L_{BC}^{eq} = L_{BB} + L_{CC} - 2L_{BC} \\ L_{CA}^{eq} = L_{CC} + L_{AA} - 2L_{CA} \end{cases} \tag{5}$$

In addition, according to [15], the self- and mutual- inductance can be expressed as:

$$\begin{cases} L_{AA} = \frac{2}{3}(L_1 + L_2\cos 2\theta); \\ L_{AB} = \frac{2}{3}\left[-\frac{L_1}{2} + L_2\cos\left(2\theta - \frac{2}{3}\pi\right)\right]; \\ L_{AC} = \frac{2}{3}\left[-\frac{L_1}{2} + L_2\cos\left(2\theta + \frac{2}{3}\pi\right)\right]; \\ L_{BA} = \frac{2}{3}\left[-\frac{L_1}{2} + L_2\cos\left(2\theta - \frac{2}{3}\pi\right)\right]; \\ L_{BB} = \frac{2}{3}\left[L_1 + L_2\cos\left(2\theta - \frac{4}{3}\pi\right)\right]; \\ L_{BC} = \frac{2}{3}\left(-\frac{L_1}{2} + L_2\cos 2\theta\right); \\ L_{CA} = \frac{2}{3}\left[-\frac{L_1}{2} + L_2\cos\left(2\theta + \frac{2}{3}\pi\right)\right]; \\ L_{CB} = \frac{2}{3}\left(-\frac{L_1}{2} + L_2\cos 2\theta\right); \\ L_{CC} = \frac{2}{3}\left[L_1 + L_2\cos\left(2\theta + \frac{4}{3}\pi\right)\right]; \end{cases} \quad (6)$$

In which $L_1 = (L_d + L_q)/2$, $L_2 = (L_d - L_q)/2$ (L_d and L_q are the d-axis and q-axis inductance in the PMSM), and θ is the rotor location angle.

Substituting expressions (6) into (5), line-to-line inductances L_{AB}^{eq}, L_{BC}^{eq}, and L_{CA}^{eq} can be further simplified as:

$$\begin{cases} L_{AB}^{eq} = 2L_1 - 2L_2\cos\left(2\theta - \frac{2\pi}{3}\right) \\ L_{BC}^{eq} = 2L_1 - 2L_2\cos 2\theta \\ L_{CA}^{eq} = 2L_1 - 2L_2\cos\left(2\theta + \frac{2\pi}{3}\right) \end{cases} \quad (7)$$

It can be seen from (7) that the line-to-line inductance of any two phase is a function of the rotor location angle θ. Thus, the values of the inductance depend on the rotor location at standstill. This phenomenon is not same as the induction motor. In practice, the rotor location is an uncertain parameter at a standstill, leading to the measured line-to-line inductance uncertainty.

3. Line-to-Line Resistance and Inductance Analysis for Stator Fault

3.1. Line-to-Line Resistance Analysis

When the stator inter-turn short circuit fault occurs in phase A, an extra branch with resistance R_f is added to the fault part of phase A. Accordingly, the DC equivalent circuit of the motor is shown in Figure 3, where R_f represents an additional resistance between the shorted turns, η represents the fault severity and $\eta = n_{cc}/N_s$ (n_{cc} is the number of the shorted turns and N_s is the total number of stator windings).

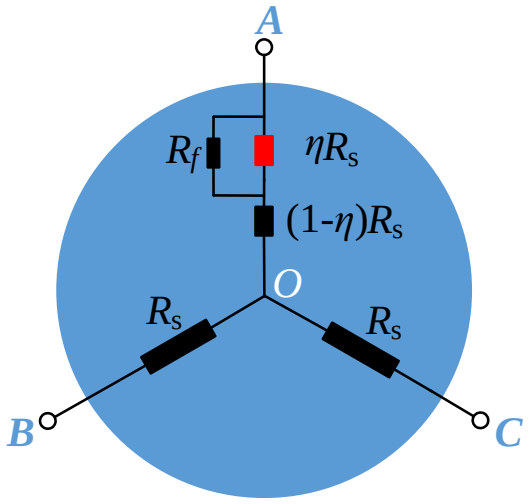

Figure 3. DC equivalent circuit when the motor has stator fault.

According to the equivalent circuit, the stator resistance of three phases can be written as:

$$R_{\mathrm{A}} = \frac{R_f \times \eta R_{\mathrm{s}}}{R_f + \eta R_{\mathrm{s}}} + (1-\eta)R_{\mathrm{s}} \tag{8}$$

$$R_{\mathrm{B}} = R_{\mathrm{C}} = R_{\mathrm{s}} \tag{9}$$

Hence, when a DC voltage is supplied to the fault motor, the line-to-line resistance of any two phases is further deduced and simplified as:

$$\begin{cases} R_{\mathrm{AB}} = R_{\mathrm{CA}} = 2R_{\mathrm{s}} - \frac{\eta^2 R_{\mathrm{s}}^2}{R_f + \eta R_{\mathrm{s}}} \\ R_{\mathrm{BC}} = 2R_{\mathrm{s}} \end{cases} \tag{10}$$

By comparing Equation (10) to (1), it can be seen that R_{AB} and R_{CA} in the stator fault motor are less than those in the healthy motor.

3.2. Line-to-Line Inductance Analysis

The motor equivalent circuit under the high-frequency AC excitation when phase A has a stator inter-turn short fault is shown in Figure 4, where the AC voltage is applied to phase A and B.

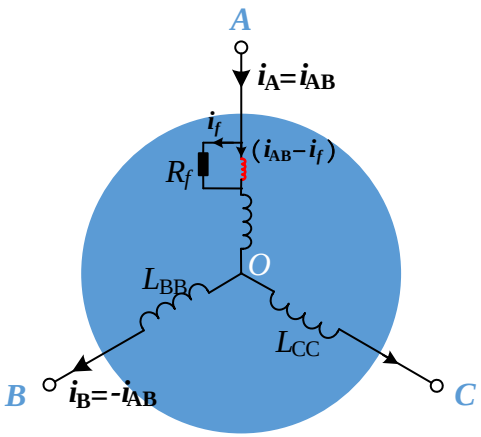

Figure 4. AC equivalent circuit of the stator fault, where the fault occurs in phase A and i_f is the current that flows through the fault part.

According to the circuit, the phases A and B flux can be written as:

$$\begin{cases} \psi_{\mathrm{A}} = \eta^2 L_{\mathrm{AA}}\left(i_{\mathrm{AB}} - i_f\right) + (1-\eta)^2 L_{\mathrm{AA}} i_{\mathrm{AB}} + \eta(1-\eta)L_{\mathrm{AA}}\left(i_{\mathrm{AB}} - i_f\right) + \eta(1-\eta)L_{\mathrm{AA}} i_{\mathrm{AB}} - [\eta L_{\mathrm{AB}} i_{\mathrm{AB}} + (1-\eta)L_{\mathrm{AB}} i_{\mathrm{AB}}] \\ \psi_{\mathrm{B}} = \left[\eta L_{\mathrm{AB}}\left(i_{\mathrm{AB}} - i_f\right) + (1-\eta)L_{\mathrm{AB}} i_{\mathrm{AB}}\right] - L_{\mathrm{BB}} i_{\mathrm{AB}} \end{cases} \tag{11}$$

The above formula can be further simplified as:

$$\begin{cases} \psi_{\mathrm{A}} = L_{\mathrm{AA}} i_{\mathrm{AB}} - L_{\mathrm{AB}} i_{\mathrm{AB}} - \eta L_{\mathrm{AA}} i_f \\ \psi_{\mathrm{B}} = L_{\mathrm{AB}} i_{\mathrm{AB}} - L_{\mathrm{BB}} i_{\mathrm{AB}} - \eta L_{\mathrm{AB}} i_f \end{cases} \tag{12}$$

Hence, the line-to-line inductance of the stator fault can be calculated as:

$$L_{\mathrm{AB}}^{\mathrm{eq}} = L_{\mathrm{AA}} - 2L_{\mathrm{AB}} + L_{\mathrm{BB}} - \eta(L_{\mathrm{AA}} - L_{\mathrm{AB}})\frac{i_f}{i_{\mathrm{AB}}} \tag{13}$$

Similarly, when the stator fault occurs in phase A, the line-to-line inductance of any two phases can be derived as:

$$\begin{cases} L_{\mathrm{AB}}^{\mathrm{eq}} = L_{\mathrm{AA}} - 2L_{\mathrm{AB}} + L_{\mathrm{BB}} - \eta(L_{\mathrm{AA}} - L_{\mathrm{AB}})\frac{i_f}{i_{\mathrm{AB}}} \\ L_{\mathrm{BC}}^{\mathrm{eq}} = L_{\mathrm{BB}} + L_{\mathrm{CC}} - 2L_{\mathrm{BC}} \\ L_{\mathrm{CA}}^{\mathrm{eq}} = L_{\mathrm{AA}} - 2L_{\mathrm{CA}} + L_{\mathrm{CC}} - \eta(L_{\mathrm{AA}} - L_{\mathrm{CA}})\frac{i_f}{i_{\mathrm{CA}}} \end{cases} \tag{14}$$

Obviously, when the stator fault occurs in phase A, the phase-A-related inductances $L_{\mathrm{AB}}^{\mathrm{eq}}$ and $L_{\mathrm{CA}}^{\mathrm{eq}}$ are not same as the healthy condition. Furthermore, the line-to-line inductance are simplified as:

$$\begin{cases} L_{\mathrm{AB}}^{\mathrm{eq}} = 2L_1 - 2L_2\cos\left(2\theta - \frac{2}{3}\pi\right) - \eta\left(L_1 - 2\frac{\sqrt{3}}{3}L_2\sin\left(2\theta - \frac{\pi}{3}\right)\right)\frac{i_f}{i_{\mathrm{AB}}} \\ L_{\mathrm{BC}}^{\mathrm{eq}} = 2L_1 - 2L_2\cos 2\theta \\ L_{\mathrm{CA}}^{\mathrm{eq}} = 2L_1 - 2L_2\cos\left(2\theta + \frac{2}{3}\pi\right) - \eta\left(L_1 + 2\frac{\sqrt{3}}{3}L_2\sin\left(2\theta + \frac{\pi}{3}\right)\right)\frac{i_f}{i_{\mathrm{CA}}} \end{cases} \tag{15}$$

For a permanent magnet synchronous motor, $L_{\mathrm{d}} \leq L_{\mathrm{q}}$, and then it can be obtained that $(L_1 - 2\sqrt{3}L_2/3) > 0$. Therefore, when the stator fault occurs, the fault-phase-related inductance decreases compared to the healthy motor.

4. Detection and Evaluation for the Stator Fault

According to the above analysis, when the motor has a stator fault, the line-to-line resistance and inductance of the fault phase decrease. On this basis, the stator fault can be detected by evaluating the resistance and inductance.

Firstly, it can be seen from (10) that the three-phase resistances are unbalance for stator fault, thus the unbalance of the resistance can be adopted as a fault indicator.

$$\mathrm{FI}^{\mathrm{R}} = \frac{\max(R_{\mathrm{AB}}, R_{\mathrm{BC}}, R_{\mathrm{CA}}) - \mathrm{average}(R_{\mathrm{AB}}, R_{\mathrm{BC}}, R_{\mathrm{CA}})}{\mathrm{average}(R_{\mathrm{AB}}, R_{\mathrm{BC}}, R_{\mathrm{CA}})} \times 100\% \tag{16}$$

Additionally, when the stator fault occurs, the line-to-line resistance of the fault phase will decrease, which provides a new parameter to evaluate the stator fault severity and location:

$$\mathrm{FI}^{\Delta\mathrm{R}} = \frac{(R_{x0} - R_x)}{R_{x0}} \times 100\% \tag{17}$$

where the R_{x} represents the new measured line-to-line resistance, which can be one of R_{AB}, R_{BC} and R_{CA}; R_{x0} represents corresponding initial line-to-line resistance.

As the inductances are the function of rotor location, the three-phase inductances are different from each other for an un-known rotor position θ even in a healthy motor; thus the unbalance of the inductances cannot be used as the fault index. On the other hand, it can be seen from (7) that the sum of the inductances is a constant of $6L_1$, which is independent of the rotor position θ. For a stator fault motor, the sum of the inductances can be derived as:

$$L_{\mathrm{ABC}}^{\mathrm{eq}} = \underbrace{6L_1}_{\text{health part}} - \underbrace{\left[\eta\left(L_1 - 2\frac{\sqrt{3}}{3}L_2\sin\left(2\theta - \frac{\pi}{3}\right)\right)\frac{i_f}{i_{\mathrm{AB}}} + \eta\left(L_1 + 2\frac{\sqrt{3}}{3}L_2\sin\left(2\theta + \frac{\pi}{3}\right)\right)\frac{i_f}{i_{\mathrm{CA}}}\right]}_{\text{fault part}} \tag{18}$$

where $L_{\mathrm{ABC}}^{\mathrm{eq}}$ is the sum of the measured line-to-line inductances. Therefore, it defines the difference of the inductance $L_{\mathrm{ABC}}^{\mathrm{eq}}$ before and after the stator fault occurs as the fault feature:

$$\mathrm{FI}^{\Delta\mathrm{L}} = \frac{\left(L_{\mathrm{ABC0}}^{\mathrm{eq}} - L_{\mathrm{ABC}}^{\mathrm{eq}}\right)}{L_{\mathrm{ABC0}}^{\mathrm{eq}}} \times 100\% \tag{19}$$

in which L_{ABC0}^{eq} is the sum of the initial line-to-line inductance.

In summary, when the stator fault occurs, the resistance and inductance will decrease. On this basis, this paper defines three fault indicators—FI^R, $FI^{\Delta R}$, and $FI^{\Delta L}$—and then the stator fault can be further detected and located through the evaluation of the fault indicators.

5. Experiment

5.1. Tested PMSM with the Stator Fault Injection

To obtain a motor with a stator fault, it damages the insulation of some windings, and then takes out some terminals of these windings to the outsides with taps, as shown in Figure 5. Hence, the stator fault can be provided through shorting these additional taps. The nominal parameters of the tested motor are presented in Table 1.

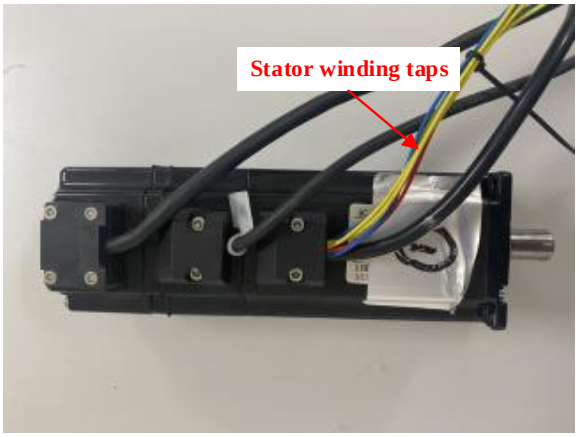

Figure 5. PMSM with the stator inter-turn short fault injection.

Table 1. Motor parameters.

Parameters	Values
Rated power/(W)	400
Rated voltage/(V)	220
Rated current/(A)	2.8
Rated speed/(rpm)	3000
Rated torque/(N.m)	1.27
Line-to-line resistance/(Ω)	3.43
Line-to-line inductance/(mH)	6.6
Inertia/(kg/m^2 × 10^{-4})	0.32

The motor has three coils in a phase, and there are 56 turns in a coil. To obtain different fault severities, it takes out the 1st, 3rd, 6th, 8th, 16th turns of the first coil of phase A to the outside. Accordingly, the number of the shorted turn can be 2, 3, 5, 7, 8, 10, 13, and 15.

5.2. Test Results

It changes the turns that are shorted in the test, and thus the number of the shorted turns changes. Therefore, the line-to-line resistance and inductance under different fault severities can be obtained through the measurements of a LCR meter. Here, the LCR meter can provide the DC and AC voltage to the motor, and then display the measured resistance and inductance values.

The measured line-to-line resistance and inductance under different numbers of shorted turns are shown in Table 2, where the inductance values shown in the table are obtained under the same rotor location. To better observe the resistance and inductance under different fault severities, the resistance and inductance are performed, as the curves shown in Figures 6 and 7, respectively.

Table 2. Measured resistance and inductance.

The Number of Shorted Turns	Line-to-Line Resistance/(Ω)			Line-to-Line Inductance/(mH)		
	R_{AB}	R_{BC}	R_{CA}	L_{AB}^{eq}	L_{BC}^{eq}	L_{CA}^{eq}
health	2.8345	2.8490	2.8480	7.4559	7.3719	7.3049
2 turns	2.8310	2.8480	2.8440	6.5480	7.3425	6.6970
3 turns	2.8260	2.8493	2.8400	6.0690	7.3200	6.4120
5 turns	2.8170	2.8487	2.8260	5.7000	7.3067	6.1410
7 turns	2.8020	2.8497	2.8120	5.5250	7.2980	6.0580
8 turns	2.8000	2.8490	2.8100	5.4370	7.2940	6.0026
10 turns	2.7760	2.8490	2.7890	5.3840	7.2919	5.9718
13 turns	2.7580	2.8490	2.7645	5.3150	7.2890	5.9254
15 turns	2.7360	2.8494	2.7490	5.2970	7.2880	5.9174

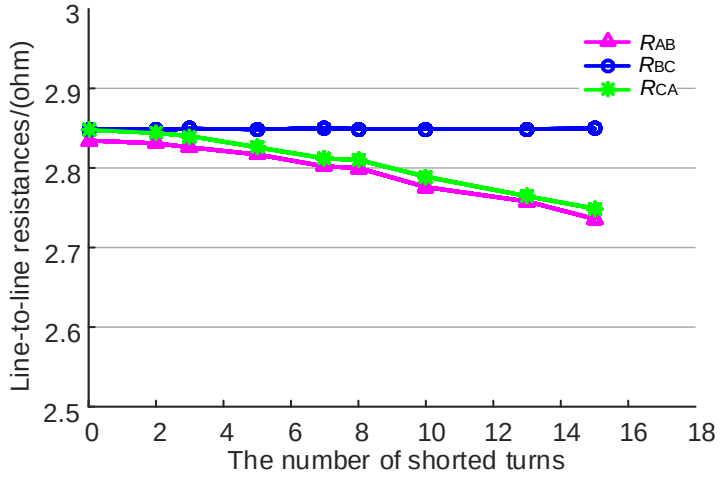

Figure 6. Line-to-line resistance under different numbers of the shorted turns.

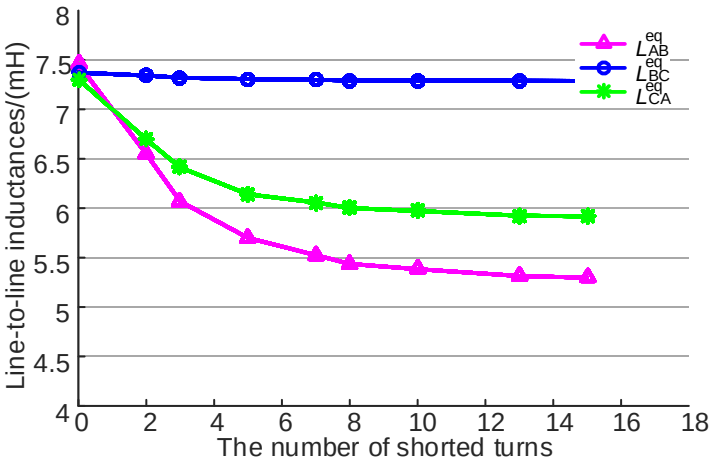

Figure 7. Line-to-line inductance under different numbers of the shorted turns.

We can see that the measured resistances and inductances in Table 2 are different from the rated parameters shown in Table 1. For resistances, this is because the resistance shown in Table 2 is measured under ambient temperature, whereas resistance in Table 1 is obtained

under 75 °C. For inductances, according to the above analysis, the line-to-line inductance changes with rotor location, and thus, the inductance value depends on rotor location.

The measured resistances shown in Table 2 are described as the curves shown in Figure 6. It can be seen from the figure that when the stator fault occurs in phase A, both R_{AB} and R_{CA} decrease with the increasing the number of the shorted turns, whereas R_{BC} is almost unchanged. Similarly, as shown in Figure 7, when the number of the shortened turns increases, the line-to-line inductances L_{AB}^{eq} and L_{CA}^{eq} decrease, whereas L_{BC}^{eq} is constant. Comparing Figures 6 and 7, it can be seen that the fault inductances drop sharply relatively to the resistances. This phenomenon reflects that the stator fault has a greater influence on the inductance than resistance, which indicates that inductance is an excellent parameter to recognize the stator fault.

According to Equations (16) and (17), the stator fault indicators FI^{R} and $FI^{\Delta R}$ can be calculated through the measured data. These two fault indicators under different fault severities are performed, as the curves shown in Figures 8 and 9. In Figure 8, the fault indicator FI^{R} increases with the number of shorted turns from 0.182% to 2.565%. Figure 9 shows that the fault indicators $FI^{\Delta RAB}$ and $FI^{\Delta RBC}$ increase from 0% to 3.475%, whereas $FI^{\Delta RCA}$ is almost unchanged (nearly 0), which indicates that phases B and C are healthy and phase A has a stator fault. Therefore, the fault indicator FI^{R} can determine whether the motor has a stator fault, and the $FI^{\Delta RAB}$, $FI^{\Delta RBC}$, and $FI^{\Delta RCA}$ can identify the fault phase.

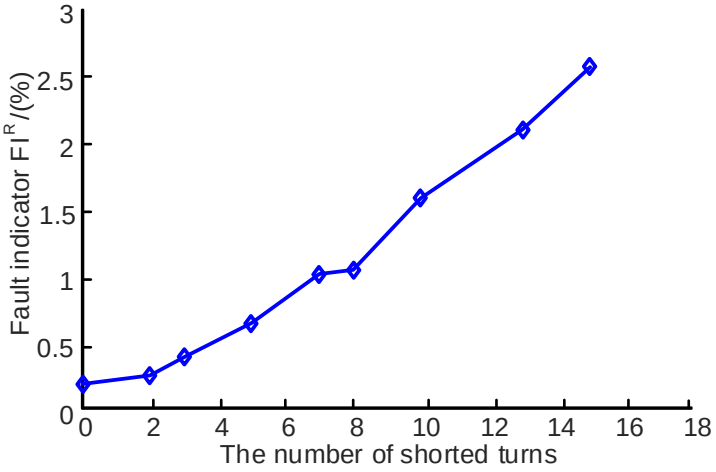

Figure 8. FI^{R} under different numbers of the shorted turns.

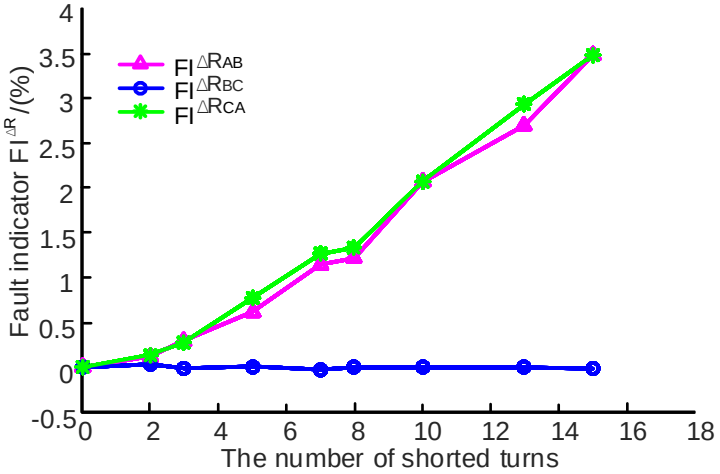

Figure 9. $FI^{\Delta R}$ under different numbers of the shorted turns.

In addition, the fault indicator of the line-to-line inductance $FI^{\Delta L}$ can be calculated through Equation (19), and the calculation results are drawn as the curve shown in Figure 10, where $FI^{\Delta L}$ increases from 0% to 16.4%, which changes significantly compared to the resistance fault indicator $FI^{\Delta R}$.

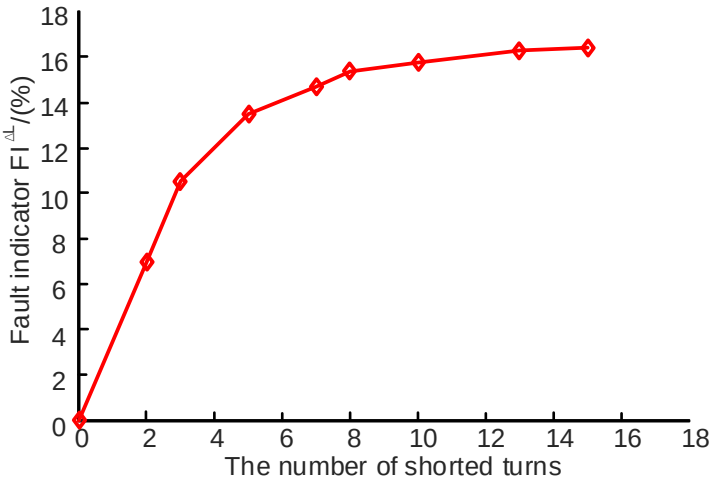

Figure 10. $FI^{\Delta L}$ under different numbers of shorted turns.

In summary, when the stator fault occurs in phase A, the line-to-line resistances R_{AB}, R_{CA} and the inductances L_{AB}^{eq}, L_{CA}^{eq} increase with the number of the shorted turns, whereas the R_{BC} and L_{BC}^{eq} are almost unchanged, which is in agreement with the proposed algorithm in this paper. Correspondingly, the resistance fault indicators FI^{R} and $FI^{\Delta R}$ have different degrees of change, which can be adopted to detect the stator fault and locate the fault phase. Compared with the resistance fault indicator, the inductance fault indicator $FI^{\Delta L}$ increases obviously, which is valuable for stator fault diagnosis.

6. Conclusions

A stator fault detection method based on the line-to-line resistance and inductance analysis is introduced and validated in this paper. The resistance and inductance of healthy and faulty motors are analyzed and compared. On this basis, three fault indicators, FI^{R}, $FI^{\Delta R}$ and $FI^{\Delta L}$, are proposed to detect and locate the stator fault. The test results of a 400 W PMSM under different fault severities lead to the following conclusions:

1. When a stator fault occurs, the line-to-line resistance and inductance related to the fault phase decrease, whereas the others are unchanged.
2. The fault indicator FI^{R} that represents the imbalance of the resistances increases with the number of shorted turns, which can be used to detect the stator fault.
3. The fault indicator $FI^{\Delta R}$ describes the rate of resistance change. When a stator fault occurs, the $FI^{\Delta R}$ related to the fault phase increases, whereas the other is nearly 0, which can provide a powerful basis to detect and locate the stator fault.
4. The fault indicator $FI^{\Delta L}$ increases significantly when the motor has a stator fault, which is valuable for stator fault diagnosis.

In actual implementation, it can measure the resistances and inductances firstly. Then the three fault indicators can be calculated through the above fault indicators definition. Moreover, the stator fault can be estimated by comparing fault indicators FI^{R}, $FI^{\Delta R}$, and $FI^{\Delta L}$ to their thresholds. Here, the stator fault has a great influence on the fault indicator $FI^{\Delta L}$, so it can obtain an excellent fault diagnosis result by using the $FI^{\Delta L}$. Compared to the online method, the offline method proposed in this paper has the advantage of easily implementation and high accuracy.

Author Contributions: All authors contributed to this work. Conceptualization, J.T. and Y.W.; methodology, J.T. and Y.W.; validation, J.T., C.L., S.L. and J.Z.; writing—original draft, J.T. and Y.W.; writing—review and editing, C.L. All authors have read and agreed to the published version of the manuscript.

Funding: This research was funded by 2019 High-quality Development Special Project of Ministry of Industry and Information Technology (TC19084DZ/2), 2019 Industrial Technology Basic Public Service Platform Project of Ministry of Industry and Information Technology (No. 2019-00896-3-1), and Development Fund Project of China CEPREI Laboratory (19Z13).

Institutional Review Board Statement: Not applicable.

Informed Consent Statement: Not applicable.

Data Availability Statement: Not applicable.

Conflicts of Interest: The authors declare no conflict of interest.

References

1. Qi, Y.; Bostanci, E.; Zafarani, M.; Akin, B. Severity Estimation of Interturn Short Circuit Fault for PMSM. *IEEE Trans. Ind. Electron.* **2019**, *66*, 7260–7269. [CrossRef]
2. Hang, J.; Zhang, J.; Cheng, M.; Huang, J. Online Interturn Fault Diagnosis of Permanent Magnet Synchronous Machine Using Zero-Sequence Components. *IEEE Trans. Power Electron.* **2015**, *30*, 6731–6741. [CrossRef]
3. Motor Reliability Working Group. Report of large motor reliability survey of industrial and commercial installations: Part I. *IEEE Trans. Ind. Appl.* **1985**, *IA-21*, 1985. [CrossRef]
4. Motor Reliability Working Group. Report of large motor reliability survey of industrial and commercial installations: Part II. *IEEE Trans. Ind. Appl.* **1985**, *IA-21*, 9533. [CrossRef]
5. Ukil, A.; Chen, S.; Andenna, A. Detection of stator short circuit faults in three-phase induction motors using motor current zero crossing instants. *Electr. Power Syst. Res.* **2011**, *81*, 1036–1044. [CrossRef]
6. Zheng, D.; Zhang, P. An Online Groundwall and Phase-to-Phase Stator Insulation Monitoring Method for Inverter-Fed Machine. *IEEE Trans. Ind. Electron.* **2021**, *68*, 5303–5313. [CrossRef]
7. Liu, T. Research on Stator Winding Interturn Short Circuit Faults Diagnosis of Induction Motor. Ph.D. Thesis, Zhejiang University, Zhejiang, China, 2007.
8. Briz, F.; Degner, M.W.; Zamarron, A. Online Stator Winding Fault Diagnosis in Inverter-Fed AC Machines using High-Frequency Signal Injection. *IEEE Trans. Ind. Appl.* **2003**, *39*, 1109–1117. [CrossRef]
9. Cheng, S.; Zhang, P.; Habetler, T.G. An Impedance Identification Approach to Sensitive Detection and Location of Stator Turn-to-Turn Faults in a Closed-Loop Multiple-Motor Drive. *IEEE Trans. Ind. Electron.* **2011**, *58*, 1545–1554. [CrossRef]
10. Ghate, V.N.; Dudul, S.V. Cascade Neural-Network-Based Fault Classifier for Three-Phase Induction Motor. *IEEE Trans. Ind. Electron.* **2011**, *58*, 1555–1563. [CrossRef]
11. Devi, N.R.; Sarma, D.V.S.S.S.; Rao, P.V.R. Diagnosis and classification of stator winding insulation faults on a three-phase induction motor using wavelet and MNN. *IEEE Trans. Dielectr. Electr. Insul.* **2016**, *23*, 2543–2555. [CrossRef]
12. Seera, M.; Lim, C.P.; Ishak, D. Fault Detection and Diagnosis of Induction Motors Using Motor Current Signature Analysis and a Hybrid FMM–CART Model. *IEEE Trans. Neural Netw. Learn. Syst.* **2012**, *23*, 97–108. [CrossRef] [PubMed]
13. Maitre, J.; Bouchard, B.; Bouzouane, A. Classification Algorithms Comparison for Interturn Short-Circuit Recognition in Induction Machines Using Best-Fit 3-D-Ellipse Method. *Can. J. Electr. Comput. Eng.* **2017**, *40*, 255–265. [CrossRef]
14. Tallam, R.M. A Survey of Methods for Detection of Stator-Related Faults in Induction Machines. *IEEE Trans. Ind. Appl.* **2007**, *43*, 920–933. [CrossRef]
15. Krishnan, R. *Permanent Magnet Synchronous and Brushless DC Motor Drives*; CRC Press, Taylor & Francis Group LLC: Boca Raton, FL, USA, 2010; ISBN 978-0-8247-5384-9.